

Molecular Docking, In-Vitro Antimicrobial, Antioxidant, and DNA Cleavage Studies of Bis-Coumarin Pyridine Schiff Basemetal Chelates

^aGeetaDnyandev Navi, ^bLatha M S, ^cVirupaxappa S Betageri, ^dVinod H Naik

^aDepartment of Chemistry Viswesaraya Technological University Belagavi

^bDepartment of PG Studies in Chemistry, Adikavi Sri Maharshi Valmiki University, Raichur -584104, Karnataka, India

^cDepartment of Chemistry, GMITDavanagere affiliated to VTU Belagavi

^dDepartment of Chemistry KLS's Vishwanathrao Deshpande Institute of Technology Haliyal Uttar Kannada, India

*Corresponding author: Dr. Vinod H Naik VDIH Haliyal

Abstract: Bis-CoumarinPyridine Schiff basederivative **3**(BCPS) metal chelates with hydroxyl functionality on both sides of the coumarin benzene ring of ML.H₂O, containing Co (II), Ni (II) and Cu (II) compounds were designed and synthesized by condensation of 2,6-diamino Pyridine and 5-formyl-6-hydroxy coumarin, the compounds are non-electrolytes and are DMSO and DMF soluble. Compounds that were synthesized were characterized using a variety of analytical methods, such as FT-IR, ¹H-NMR, ¹³C-NMR, ESI-MS, and EPR analysis. Coumarins and Schiff bases share an interest in medicinal chemistry because they can have pharmacological effects. Similarly, the target molecules' bio-potency was tested in vitro for antimicrobial (E. coli, S. aureus, P. aeruginosa, and S. typhi) and antifungal (Aspergillus Niger, Aspergillus flavus, and Cladosporium) activity, and the agarose gel electrophoresis technique was used to investigate DNA cleavage, as well as antioxidant properties, which confirmed their promising biological activities when compared to standard drugs.

Keywords: Bis-CoumarinPyridine , pharmacological, Cladosporium.

Introduction:

Because of their numerous uses in chemistry, biology, agrochemistry, and phytosanitary activities, heterocyclic compounds are important for the synthesis of Schiff bases [1-3]. As a result, a wide range of pharmacological uses and reactions in heterocyclic compounds have been demonstrated to play an important role in heterocyclic chemistry. Schiff bases are heterocyclic chemical derivatives that have gained prominence due to their range of applications. A six-membered organic heterocyclic compound Pyridine, having an unsaturated ring structure with nitrogen [4-7] and Coumarin compounds, has a broad spectrum of usage; the biochemical action of the coumarin nucleus and associated compounds has a considerable influence on many physicochemical properties, quenching of

reactive oxygen species, as well as antitumorigenic and plant development regulators [8, 9].

Apart from these, they are extensively utilized as food ingredients, fragrances, cosmetics, and pharmaceuticals, as well as in manufacturing pesticides, visual brighteners, and fluorescent and laser pigments [10-12]. These results have fascinated many chemists to work on this heterocyclic core. Coumarins were made through various methods, including Wittig, Reformatsky, and Knoevenagel reactions [13-18]. 2,6-Diamino-pyridine is a medium-production-volume compound used in oxidation/permanent formulas as a medicinal intermediate for drug synthesis [21-24]. In association with transition metal compounds with DNA, they are widely investigated for their possible application markers for DNA structure and treatment. Recent evidence

points to a role for Cu (II) molecules in DNA segment scission [23-25]. Scrounging the steady DPPH radical model is a popular technique for evaluating antioxidant actions, and it is a comparatively fast approach to any alternative method. The capacity of antioxidants to contribute hydrogen was believed to be responsible for their impact on DPPH radical scavenging [26]. The reactions of chemically associated flavonoids (quercetin, kaempferol, rutin, and luteolin) with Cu⁺ ions are studied by complex creation *via* chelation or alteration *via* oxidation, in addition to structural reliance. The ortho hydroxy group in the B ring is essential for creating Cu⁺ chelates, which increase antioxidant action.

The rationality of the design and synthesis of Schiff bases has drawn the attention of researchers to identify the chemically modified structures for their enhanced bioactivity and antibiotic resistance for the concern of global health. Oxidative stress-related disorders continue to be a considerable burden, and Schiff bases have emerged as a viable possibility for treating bacterial infections and preventing oxidative damage in innovative therapeutic treatments. This opening paragraph intends to shed light on the compelling grounds for using Schiff bases in medicine and therapeutic interventions as powerful dual-function agents in the fight against bacterial infections and oxidative stress-related diseases.

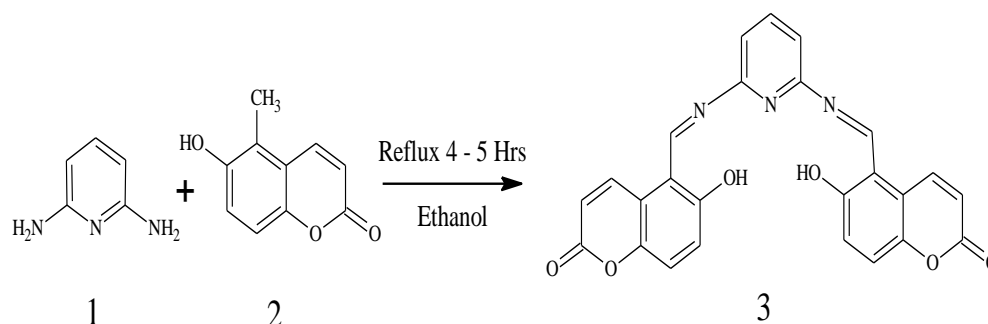
As an extension of our prior research on Schiff's base metal complexes [27-29], this present article emphasizes the antibacterial, antioxidant, and DNA cleavage actions of pyrimidine-derived Schiff bases of a metal chelate of Cobalt (II), Nickel (II), and Copper (II) are obtained from 2,6-diamino Pyridine and 5-Formyl-6-hydroxy coumarin. Thus, numerous spectral and chemical techniques are utilized to explore the molecular topographies of derivatives.

In support of this, in-silico Bioinformatics techniques were used to conduct molecular docking studies on the target compounds in order to better understand their physiological features and drug-receptor interactions. In general, the conventional synthetic approaches of these molecules, their versatility, and their wide range of applications mark them substantial. As a result, the present

investigation, especially heterocyclic composites, has attracted the enormous attention of chemical researchers in the current scenario.

2.1 Materials and Methods : Chemicals of laboratory quality were obtained, and 6-hydroxy coumarin [30] and 5-formyl-6-hydroxy coumarin [31,32] were synthesised following the published technique. The Carlo Erba EA1108 Chemical Analyzer calculates the presence of Carbon, Hydrogen, and Nitrogen compounds. The IR spectra of the Schiff bases were also captured using an HITACHI-270 spectrophotometer. The electronic spectra of the target molecules were obtained at 200-1100 nm using a VARIAN CARY 50-BIO UV spectrophotometer in HPLC grade DMF and DMSO solvent. The ¹H-NMR and ¹³C spectra of ligands were recorded at room temperature using a BRUKER 300 MHz spectrometer with TMS as an internal reference in D₆-DMSO. FAB-mass spectra were obtained utilising an Argon/Xenon (6KV, 10 Am) FAB gas on a JEOL SX 102/DA-6000 mass spectrometer/data system in the positive ion phase. The external stimulation was 10 KV, and the spectra were recorded in RT using m-nitrobenzylalcohol. The electrochemistry of complexes was studied using a CHI110A Electrochemical Analyzer (Made in USA) in dimethyl formamide (DMF) with 0.05 M n-Bu₄NClO₄ as a supplementary material. The ESR spectra was captured using a Varian E-4X-band EPR spectrometer. Thermogravimetric measurements were taken from room temperature to 1000°C at 10 °C/min. The data was collected using a TA TG/DTA instrument. Molar conductivity measurements were obtained on the ELICO-CM-82 T Conductivity Bridge using a cell with a cell constant of 0.51, while magnetic moment measurements were taken with a Faraday balance.

2.2 Schiff Base Preparation : Figure 1 depicts the schematic representation of Schiff base synthesis, a stirred solution of 2, 4 diamino pyridine 1(0.01mol) and 6-Hydroxy-5-Formyl coumarin 2(0.01mol) in ethanol 30mL for 4-5 hours with few drops of concentrated HCL. The reaction mixture was put into ice-cold water to precipitate solids, rinsed with cold EtOH, and filtered and dried. The compound was allowed recrystallization from EtOH.



5,5'-[pyridine-2,6-diylbis(azanylylidenemethanylylidene)]bis(6-hydroxy-2*H*-1-benzopyran-2-one)

Scheme 1: Design of Bis-coumarinPyridineSchiffbasederivative (BCPS)

2.3Preparation of Co(II), Ni(II) and Cu(II) complexes : 2 mmol of Schiff base compound 3 in alcoholic solution (45 mL) was mixed with 1 mmol of $\text{CoCl}_2 \cdot 6\text{H}_2\text{O}$ / $\text{NiCl}_2 \cdot 6\text{H}_2\text{O}$ / $\text{CuCl}_2 \cdot 2\text{H}_2\text{O}$ in alcoholic solution (5 mL) and refluxed in a water bath for 2 hrs. After adding 2 mmol of $\text{C}_2\text{H}_5\text{NaO}_2$, the solution was refluxed for 3 hours. The filtrate was washed with cold H_2O and $\text{C}_2\text{H}_5\text{OH}$ before vacuum-drying on melted CaCl_2 ; the separated chemical was now ready for usage.

2.4Pharmacology

2.4.1Antimicrobial Testing

2.4.1.1Culture mediapreparation : Nutrient broth [peptone, 10; yeast extract, 5; NaCl , 10; in (g/l)] was used for bacterial growth, whereas potato dextrose broth [potato, 250; dextrose, 20; in (g/l)] was used for fungal growth. The 50 cc medium was sterilised at 121°C and 15 pressure for 15 minutes. Following that, the medium was autoclaved, and the seed culture was injected [35].

2.4.1.2 In-Vitro AantimicrobialAssay:

Antimicrobial screening of synthetic Schiff bases and metallic compounds was carried out using nutrient agar and potato dextrose agar diffusion methods. The antibacterial and antifungal capabilities were examined using MIC approach on four bacteria (*E. Coli*, *S. Aureus*, *P. aeruginosa*, and *S. Typhi*) and three fungi (*A. Niger*, *A. Flavus*, and *Cladosporium*) at doses of 10, 30, 50, and 100 $\mu\text{g/mL}$ in DMF. The bacterial samples were incubated for about 24 hours at 37°C , and fungal cultures for about 3-4 days at room temperature, respectively, the results were compared under identical conditions, with an antibiotic

(Gentamycin) and an antifungal (Fluconazole) serving as standards [35].

2.4.2 DNA Cleavage Testing

2.4.2.1Method for Isolating DNA : The pellet from a fresh bacterial sample (1.5 mL) is removed by centrifugation and melted in 0.5 mL of lysis solution (100 mM tris pH 8.0, 50 mM EDTA, 10% SDS). To this solution, 0.5 millilitres of saturated phenol are added and gestated at 55°C for a few minutes. After centrifugation at 10,000 rpm for 10 minutes, an equivalent volume of chloroform:isoamyl alcohol (24:1) is added to the supernatant, along with a 1/20th measurement of 3M sodium acetate (pH 4.8). The supernatant was centrifuged at 10,000 rpm for 10 minutes, then three litres of cold absolute alcohol were added. The precipitated DNA was separated by centrifugation, and the dried pellets were reconstituted in TAE solution (10 mM tris pH 8.0, 1 mM EDTA) and kept aside at room temperature.

2.4.2.2Agarose Gel Electrophoresis: The agarose gel electrophoresis investigates the cleavage substances [33,34]. DMF was employed to generate test samples (1 mg/mL). The samples (25 μg) were mixed with *E. coli*, *P. aeruginosa*, and *A. niger* extracted DNA. The materials were kept at 37°C for 2 hours. In the electrophoresis chamber, 20 μL of DNA sample (mixed with bromophenol blue dye at a 1:1 ratio) was carefully filled into the wells, along with a standard DNA marker comprising TAE buffer (4.84 g Tri's base, pH 8.0, 0.5 M EDTA/ltr) and finally spread on an agarose gel and passed through uniform 50 V of electricity for about half an hour. Then, the compound was withdrawn and stained for 10-15 minutes using 10.0 $\mu\text{g/mL}$ of non-

radioactive marker ethidium bromide. To identify the degree of DNA fragmentation, the band's visibleness was recorded and confirmed by the Vilberlourmatemethod. The findings are then compared to conventional Genetic identifiers.

2.4.3 Antioxidant Activities: Blois approach assesses the compounds for free radical scavenging activity [36]. To summarise, a 1mL solution of 0.1 mM 2,2-Diphenyl-1-picrylhydrazyl (DPPH) in ethyl alcohol was added to trial solutions in DMSO (3 mL) at varied ratios (50-250 µg/mL). Further, this combination was thoroughly mixed and set aside at ambient temperature for 30 minutes. The spectrophotometer records the absorption wavelength (517 nm) of the compound. This reduced wavelength absorption of the reaction combination corresponds to a greater capacity for scavenging free radicals. The DPPH content (mM) in the reaction substance was computed using the standardization graph and linear regression ($R: 0.997$): $0.0003 \times \text{DPPH} - 0.0174$. The following equation explores the capacity to recover the DPPH radical: DPPH scavenging impact (%) = $(A_0 - A_1/A_0) \times 100$, where A_0 and A_1 represent the absorption of the control response and absorbance, respectively.

3. Result and Discussions: The Schiff base in ethanol generates octahedral compounds (Figure 7) with $\text{CoCl}_2 \cdot 6\text{H}_2\text{O}$ / $\text{NiCl}_2 \cdot 6\text{H}_2\text{O}$ / $\text{CuCl}_2 \cdot 2\text{H}_2\text{O}$. The compounds Co (II), Ni (II), and Cu (II) are coloured, solid, and non-hygroscopic. These

chemicals are soluble in DMF and DMSO but insoluble in typical chemical liquids. The elemental investigations show that the molecules Co (II), Ni (II), and Cu (II) exhibit a 1:2 stoichiometry of the type $\text{ML} \cdot \text{H}_2\text{O}$ (Figure 7). The molar conductance of the DMF complexes indicates that they are not electrolytic (Table 1). The complex was heated to 105°C for 120 minutes, then cooled to room temperature, placed in a desiccator, and weighed to ensure that the water molecules in the complexes were linked to the metal ions; no weight loss was observed. These findings suggest that the water molecules are linked to the metal ions. In ethanol, the Schiff base forms octahedral complexes (4-6) of $\text{CoCl}_2 \cdot 6\text{H}_2\text{O}$, $\text{NiCl}_2 \cdot 6\text{H}_2\text{O}$, and $\text{CuCl}_2 \cdot 2\text{H}_2\text{O}$. All of the Co (II), Ni (II), and Cu (II) complexes are coloured, stable, and non-hygroscopic, and may dissolve in DMF and DMSO. Table 1 demonstrates that the elemental analyses of metallic complexes have a 1:2 stoichiometry of the form MLH_2O , where L denotes a ligand. The low molar conductance values in the table indicate a non-electrolytic nature and account for any DMF complex breakage. The complexes are weighed and heated to 105°C for 120 minutes to identify the co-ordination of water molecules and the metal ion.

The material is then placed in a desiccator to cool before being reweighed. No substantial variations in the complex weight were seen. As a result, the findings imply that water molecules coexist with metal ions in the complexes.

Table 1: Experimental parameters for Schiff bases and their metallic complexes

Sl. No.	Chemical Formula	%Yield/Color	M%		C%		H%		N%		Molar conductivity $\text{Ohm}^{-1} \text{cm}^2 \text{mole}^{-1}$	μ_{eff} (BM)
			Obsd.	Calcd.	Obsd.	Calcd.	Obsd.	Calcd.	Obsd.	Calcd.		
3	$\text{C}_{25}\text{H}_{15}\text{N}_3\text{O}_6$	74%	-	-	66.12	66.22	3.15	3.31	9.14	9.33	-	-
4	$\text{Co}[\text{C}_{25}\text{H}_{13}\text{N}_3\text{O}_6\text{H}_2\text{O}]$	68%/Brown	11.11	11.17	56.44	56.81	2.58	2.84	7.82	7.95	30.15	4.52
5	$\text{Ni}[\text{C}_{25}\text{H}_{13}\text{N}_3\text{O}_6\text{H}_2\text{O}]$	67%/Yellowish green	11.34	11.00	56.44	56.92	2.37	2.46	7.42	7.96	26.78	2.86

6	Cu[C ₂₅ H ₁₃ N ₃ O ₆ H ₂ O]	65%/Dark green	11.12	11.84	56.13	56.39	2.44	2.49	7.88	7.89	24.14	1.78
---	--	----------------	-------	-------	-------	-------	------	------	------	------	-------	------

3.1 IR Spectral Studies. Table 2:IR frequencies of Schiff bases and metal complexes (measured in cm⁻¹).

Compound	ν (CH=N)	ν (C=N)	ν (C=O)	ν (C-O)	ν (M-N)	ν (M-O)
C ₂₅ H ₁₅ N ₃ O ₆	1663	1605	1714	1256	-	-
Co[C ₂₅ H ₁₃ N ₃ O ₆ H ₂ O]	1641	1580	1712	1335	430	490
Ni[C ₂₅ H ₁₃ N ₃ O ₆ H ₂ O]	1640	1579	1714	1333	434	488
Cu[C ₂₅ H ₁₃ N ₃ O ₆ H ₂ O]	1635	1580	1716	1339	435	489

Table 2 signposts the protuberant IR spectral values of samples. The Schiff base **3** IR spectra revealed a typical line caused by ν (CH=N) appearing in 1663 cm⁻¹. Further ν (C=N) is given the distinctive high-intensity band in the area 1605 cm⁻¹ [37]. The phenolic (C-O) [38] and (C=O) [39] have sharp bands at 1256 and 1714 cm⁻¹ correspondingly.

In contrast to the spectroscopy of the Schiff bases and all metallic compounds showed the peak of ν (CH=N) in the range 1641-1635 cm⁻¹, this indicated the existence of the metal ion's corresponding nitrogen azomethine group in the sample [37]. It also verifies the binding of the nitrogen in the Pyridine at around 1580-1579 cm⁻¹. The appearance of peaks of moderate to considerable strength at 1339-1335 cm⁻¹ signposts ν (C-O) via deprotonation [38]. The modification of C-O on the greater side in metal complexes is owing to the complex's predicted significant mesomeric interaction, which is likely activated by the presence of the metal ion. Novel spectral lines at 430-435 cm⁻¹ and 490-488 cm⁻¹ resemble the establishment of stretching modes of (M-N) and metal-oxygen bonds correspondingly [40-41]. The unchanged peak ν

(C=O) location in all metal compounds suggests that these groups are unengaged in the co-ordination.

3.2 NMR Spectral Studies: The ¹H NMR and ¹³C NMR investigations detect all protons and carbons in both Schiff bases. Table 3 shows the NMR data for the two Schiff bases. This article describes the ¹H and ¹³C NMR spectra of a typical Schiff base. The OH proton was detected at 10.12 ppm in the Schiff base's usual ¹H NMR band (s, 2H). At 8.25 ppm, CH=N emits a unique proton signal (s, 2H). Furthermore, aromatic protons are responsible for multiplet signatures in the 7.34-7.73 ppm (m, 8H) range. The characteristic at 161 ppm in the usual ¹³C NMR profile of Schiff base I corresponds to isatinlactonyl carbon (C=O). Signals at 154.45 ppm are assigned to pyridine (C=N), whereas signals at 143.90 and 143.86 ppm are assigned to two aldimines (CH=N) groups, respectively.

Furthermore, aromatic carbon atoms are allocated to the 117.1-132.2 ppm signals. A signal at 154.45 ppm is also attributed to the Hydroxyl group at the coumarin molecule. Therefore, the NMR studies are a reliable backup to the IR conclusions.

Table 3: NMR analysis of Schiff compound

Schiff base	¹ H NMR (DMSO-d ₆) (ppm)	¹³ C NMR (DMSO-d ₆) (ppm)
C ₂₅ H ₁₅ N ₃ O ₆	10.12 (s, 2H, OH of Coumarin), 8.25 (s, 2H, CH=N) 7.34-7.73 (m, 8H, aromatic Protons)	132.22, 124.84, 127.54, (Pyridine), 154.45 (C=N), 143.86, 143.90 (CH=N), 161.45 (C=O), 123.34, 119.24, 117.30, 117.10, 117.07, 116.34, 116.21 (Coumarin).

3.3 Electronic Spectra and Magnetic Measurements: The Co (II) complex exhibited electron spectrum bands at 8000-10000 cm^{-1} and 18000-20000 cm^{-1} , which correspond to v_1 and v_3 transitions, respectively of $^4T_{1g} (F) \rightarrow ^4T_{2g} (F) (v_1)$ and $^4T_{1g} (F) \rightarrow ^4T_{1g} (P) (v_3)$. The absorbance lines at 9378 and 18213 cm^{-1} correlate to 1 as well as 3 transitions, accordingly, in the reddish Co (II) compounds studied here. All such bands are

found in intense spin octahedral Co (II) complexes [42]. Nevertheless, due to its closeness to the powerful 3 transition, the 2 band is not noticed. Table 4 displays the estimated ligand field values. Magnetic moment (μ) values of 4.52 are obtained for Co (II) compounds, which coincide with the octahedral range [43] and corroborate the electronic spectrum findings.

Table 4: Ligand field characteristics for Cobalt (II) and Nickel (II) complexes

Complex	Transitions (cm^{-1})			v_2 - Cald. cm^{-1}	$Dq \text{ cm}^{-1}$	$B^1 \text{ cm}^{-1}$	% Distortion	v_2/v_1	LSF E	μ_{eff} Cald. BM	β	$\beta^\circ \%$
	v_1	v_2	v_3									
$\text{Co}[\text{C}_{25}\text{H}_{13}\text{N}_3\text{O}_6\text{H}_2\text{O}]$	9378	-	18213	19829	1045.19	660.59	-	2.11	23.89	-	0.681	31.68
$\text{Ni}[\text{C}_{25}\text{H}_{13}\text{N}_3\text{O}_6\text{H}_2\text{O}]$	10612	16365	26441	16658	1061.20	753.26	1.994	1.54	36.38	3.166	0.713	28.67

The green $\text{Ni}[(\text{C}_{25}\text{H}_{13}\text{N}_3\text{O}_6\text{H}_2\text{O})]$ complex displayed three main bands at 10612, 16365, and 26441 cm^{-1} , which were attributed to the $^3A_{2g} \rightarrow ^3T_{2g} (v_1)$, $3A_{2g} \rightarrow ^3T_{1g} (F) (v_2)$ and $^3A_{2g} \rightarrow ^3T_{1g} (P) (v_3)$ transitions, indicating an octahedral structure around the Ni (II) ion [44]. Table 4 displays the ligand field values. The frequencies v_2/v_1 are roughly 1.44, and the μ_{eff} value is approximately 3.174, falling in the range of 2.8-3.5 BM, indicating an octahedral complex. The nephelauxetic measure β data indicate that metal-ligand interactions are minimally covalent [45, 46]. In the 2.8-3.5 BM array, Ni (II) complexes had $\mu = 2.84$, which is consistent with their octahedral surroundings [47]. As a consequence, the ligand field properties are consistent with the electronic spectrum and magnetic susceptibility measurements.

Two distinct lines may be found in the electronic spectra of Cu (II) compounds. The $^2E_g \rightarrow ^2T_{2g}$

transition is responsible for a low-intensity wide peak about 16534 cm^{-1} , whereas ligand metal charge transfer causes a high-intensity peak around 25543 cm^{-1} . Electronic spectroscopy suggests that Cu (II) ions have a twisted octahedral structure [48]. Cu (II) compounds have μ of 1.78-1.80 BM, which is somewhat higher than the spin-only value of 1.76 BM predicted for a single electron, indicating an octahedral structure [49].

3.4 FAB-Mass Spectrometry results

Figure 2 shows the usual mass spectrum of Schiff base 3, $\text{C}_{25}\text{H}_{15}\text{N}_3\text{O}_6$. The continuum showed a molecular ion peak at m/z 453, correlated with the number of molecules contained in it. Furthermore, the splinter ion spikes detected at m/z 279 and at 174 owes to $\text{C}_{10}\text{H}_6\text{O}_3$ and $\text{C}_5\text{H}_3\text{N}_3$ disintegration, correspondingly.

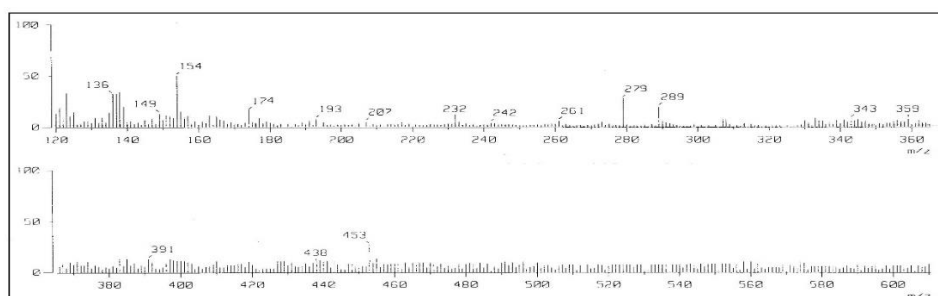


Fig.2: Mass spectrum of Schiff base 3.

The mass spectra of each compound showed molecular ion peaks and other fragmentation peaks that corresponded to their molecular weight. As a result, just its representative is addressed here (Figure 3).

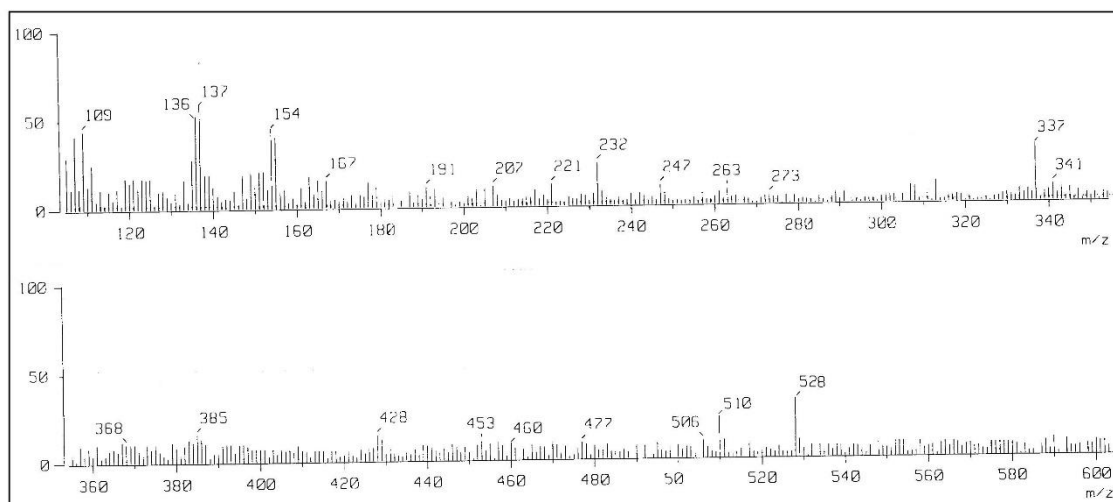


Fig. 3: Mass spectrum of $\text{Co}[\text{C}_{25}\text{H}_{13}\text{N}_3\text{O}_6\text{H}_2\text{O}]$

The continuum of $\text{Co}[(\text{C}_{25}\text{H}_{13}\text{N}_3\text{O}_6\text{H}_2\text{O})]$ reported a molecular ion peak M^+ at m/z 528. The cleavage maxima detected at 510, 337, and 232 correlate to coordinated H_2O molecules, $\text{C}_{10}\text{H}_5\text{O}_3$ and $\text{C}_5\text{H}_3\text{N}_3$. The molecular ion peak M^+ at m/z 527 is related to the molecular weight of compound $\text{Ni}[(\text{C}_{25}\text{H}_{13}\text{N}_3\text{O}_6\text{H}_2\text{O})]$. The fragmentation maxima of the complex at 509, 336, and 231 correspondingly correlate to cleavages of the coordinated water molecules, $\text{C}_{10}\text{H}_5\text{O}_3$ and $\text{C}_5\text{H}_3\text{N}_3$. The $\text{Cu}[(\text{C}_{25}\text{H}_{13}\text{N}_3\text{O}_6\text{H}_2\text{O})]$ complex spectrum includes The molecular ion peak M^+ at m/z 532 corresponds to its molecular mass.

3.5 Thermodynamic Characteristics of Metal Complexes

Thermodynamic properties of Co (II), Ni (II), and Cu (II) compounds as a function of temperature was investigated. The temperature behavior of all compounds is nearly identical. As a result, only the sample compounds $\text{Co}[(\text{C}_{25}\text{H}_{13}\text{N}_3\text{O}_6\text{H}_2\text{O})]$, $[\text{Ni}(\text{C}_{25}\text{H}_{13}\text{N}_3\text{O}_6\text{H}_2\text{O})]$ and $[\text{Cu}(\text{C}_{25}\text{H}_{13}\text{N}_3\text{O}_6\text{H}_2\text{O})]$ have been addressed.

The thermal breakdown of the compounds $\text{Co}[(\text{C}_{25}\text{H}_{13}\text{N}_3\text{O}_6\text{H}_2\text{O})]$, $[\text{Ni}(\text{C}_{25}\text{H}_{13}\text{N}_3\text{O}_6\text{H}_2\text{O})]$ and $[\text{Cu}(\text{C}_{25}\text{H}_{13}\text{N}_3\text{O}_6\text{H}_2\text{O})]$ occurs in three stages, as shown by DTG peaks at 250-260, 390-396, and 680-690 $^{\circ}\text{C}$, corresponding to the mass loss of coordinated water molecules (Fig. 4).

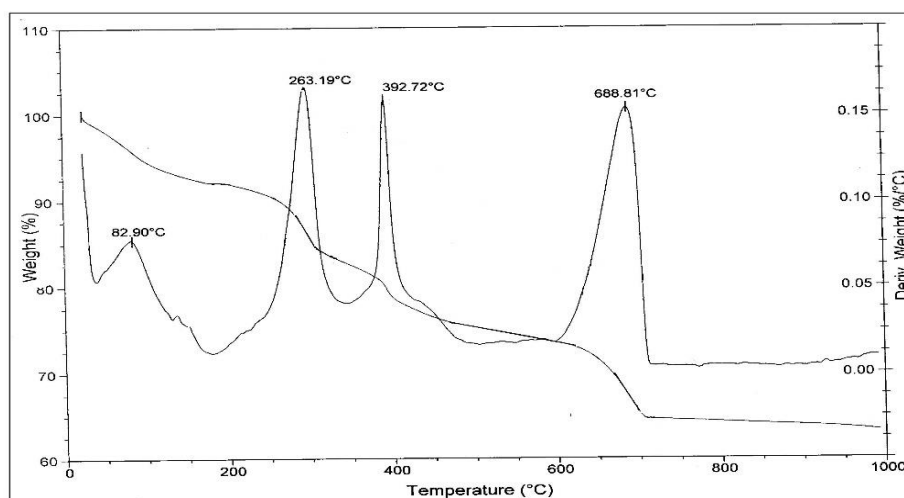


Fig. 4: TG/ DTG spectrum of the $\text{Ni}[\text{C}_{25}\text{H}_{13}\text{N}_3\text{O}_6\text{H}_2\text{O}]$.

As a result, TGA experiments corroborate the binding of water molecules with metal ions. To conclude, above 900°C, the metal compounds progressively disintegrate with a generation of metal oxide. Table 5 depicts the type of the proposed chemical shift as temperature changes and the quantity of metal oxide formed.

Table 5: Thermogravimetric parameters for complexes of Co (II), Ni (II), and Cu (II)

Molecular Formula	Melting Point (MP)	% Mass Loss		Metal Oxide %	Inference	
	°C	Obsd.	Calcd.	Obsd.	Calcd.	
Co[C ₂₅ H ₁₃ N ₃ O ₆ H ₂ O]	252-258	3.26	3.40	14.12	14.20	Loss of a coordinated water molecule
	391-393	32.83	32.78			Loss of a Coumarin moiety
	680-690	19.45	19.88			Loss of a pyridine moiety
Ni[C ₂₅ H ₁₃ N ₃ O ₆ H ₂ O]	252-259	3.23	3.41	14.34	14.04	Loss of a coordinated water molecule
	392-398	32.20	32.82			Loss of Coumarin moiety
	681-692	19.45	19.92			Loss of pyridine moiety
Cu[C ₂₅ H ₁₃ N ₃ O ₆ H ₂ O]	254-260	3.21	3.38	14.67	14.84	Loss of a coordinated water molecule
	390-394	32.44	32.51			Loss of a Coumarin moiety
	683-693	19.56	19.73			Loss of a pyridine moiety

3.6 ESR Spectrum of complex Cu[(C₂₅H₁₃N₃O₆H₂O)]

The Cu (II) complex ESR spectrum investigations detail the metal ion. Cu (II) complex ESR spectrum was acquired in DMSO at ambient temperature (LNT). The ESR spectral of one typical Cu[(C₂₅H₁₃N₃O₆H₂O)] compound is addressed in this article. Because of the rolling motion of the molecules, the spectrum at RT has an isotropic single high absorption band in the intense field area. Nevertheless, the numbers for g_{\parallel} and g_{\perp} are 2.080 and 2.012, correspondingly. These numbers imply a lone electron in the dx^2-y^2 orbital [50]. The compound $g_{\parallel} > g_{\perp} > 2.0023$ pattern suggests that the lone electron is located in the Cu (II) ion's dx^2-y^2 orbital, which is characteristic of axial symmetry. The determined g_{av} value is 2.05. As a result, the data confirmed that the Cu (II) complex possesses a twisted octahedral structure.

3.7 Pharmacological Screening

3.7.1 In-vitro antimicrobial Efficacy: The MIC approach assesses the in-vitro antibacterial capabilities of Schiff bases and their metallic compounds in comparison to seven pathogens [33]. Table 6 illustrates the inhibitory effects on bacterial development. The discovery leads to the conclusion that ligands comprising N and O donor systems may have reduced enzyme production since enzymes that enable OH groups for action appear to be more susceptible to complex ion inactivation. Compounds diffuse through the lipid layer of spore membranes to their sites of action. They eventually kill them by reacting with the OH groups of particular cell enzymes. The impermeability of the cell influences the efficacy of various biocidal substances in contrast to diverse organisms. The fractional allocation of positive charge with the ligand of chelation leads to a lowering of the polarity of the central metal atom. In addition, the creation of a hydrogen bond with the active sites of cell components via the azomethine nitrogen atom may influence the regular cell process [51].

According to the findings, metallic compounds suppress all of the microbes tested. According to the antimicrobial tests, the Schiff base is extremely energetic in contrast to *P. aeruginosa* and *S. typhi*, but only modestly dynamic counter to *E. coli* and *S. aureus*. Whole metal compounds are more antimicrobial compared to Schiff bases. Thus, the improved antibacterial activity of metal complexes over Schiff bases is due to coordinational structural

alterations, and chelating, forming metal complexes act as extra powerful and effective bacteriostatic agents, blocking microbial proliferation [52]. The study shows the minimal inhibitory concentration (MIC) of some chosen substances that exhibited considerable accomplishment counter to specific bacterial and fungal classes. Table 7 explores the fact signposting for a quantity of 10 µg/mL. It inhibits the growth of the studied organisms.

Table 6: Antimicrobial IC₅₀ values of Schiff bases metal complexes

	Conc. (µg ml ⁻¹)	% Inhibition against Bacteria				% Inhibition against Fungi		
		<i>E. coli</i>	<i>S. aureus</i>	<i>P. aeruginosa</i>	<i>S. typhi</i>	<i>A. Flavus</i>	<i>Cladosporium</i>	<i>A. Niger</i>
C₂₅H₁₅N₃O₆	10.00	15.00	13.00	14.00	18.00	32.00	40.00	38.00
	30.00	24.00	21.00	23.00	28.00	39.00	51.00	50.00
	50.00	36.00	34.00	35.00	54.00	48.00	60.00	70.00
	100.00	49.00	60.00	49.00	68.00	70.00	74.00	70.00
Co[C₂₅H₁₃N₃O₆H₂O]	10.00	18.00	26.00	24.00	27.00	50.00	45.00	44.00
	30.00	30.00	45.00	59.00	37.00	54.00	65.00	59.00
	50.00	45.00	58.00	69.00	65.00	68.00	73.00	66.00
	100.00	69.00	72.00	77.00	86.00	80.00	83.00	79.00
Ni[C₂₅H₁₃N₃O₆H₂O]	10.00	32.00	38.00	37.00	54.00	56.00	60.00	57.00
	30.00	54.00	63.00	56.00	66.00	67.00	65.00	80.00
	50.00	69.00	71.00	78.00	71.00	82.00	77.00	89.00
	100.00	84.00	85.00	90.00	84.00	88.00	89.00	90.00
Cu[C₂₅H₁₃N₃O₆H₂O]	10.00	40.00	41.00	45.00	57.00	59.00	62.00	60.00
	30.00	56.00	60.00	67.00	70.00	70.00	67.00	78.00
	50.00	73.00	74.00	74.00	88.00	75.00	81.00	85.00
	100.00	88.00	85.00	92.00	92.00	90.00	92.00	93.00
<i>Gentamycin</i>	100.00	100.00	100.00	100.00	100.00	-	-	-
<i>Fluconazole</i>	100.00	-	-	-	-	100.00	100.00	100.00

Table 7: Minimum inhibitory concentration (µg/ml) results of selected compounds.


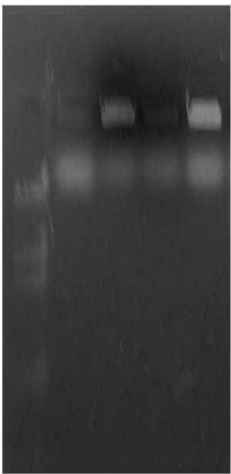
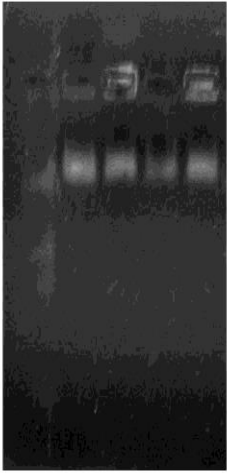
Compound	<i>E. coli</i>	<i>P. aeruginosa</i>	<i>S. Typhi</i>	<i>A. Flavus</i>	<i>Cladosporium</i>	<i>A. Niger</i>
C₂₅H₁₅N₃O₆	25.00	10.00	25.00	25.00	10.00	100.00
Co[C₂₅H₁₃N₃O₆H₂O]	25.00	10.00	25.00	10.00	25.00	100.00
Ni[C₂₅H₁₃N₃O₆H₂O]	10.00	10.00	10.00	10.00	10.00	25.00

Cu[C ₂₅ H ₁₃ N ₃ O ₆ H ₂ O]	10.00	25.00	25.00	10.00	10.00	10.00
--	-------	-------	-------	-------	-------	-------

3.8 DNA Cleavage Activity

Several agentsefficientlyinhibit the activity of enzymes on DNA. The inhibitions are caused by binding molecules to the enzyme's interaction site on DNA, rather than by direct enzyme deactivation. In general, the transition metallic elementinhibits DNA repair enzymes. The 0.8 mM Zinc chloride inhibits purified DNA ligase when moved on a

horizontal gel utilizing electrophoresis. The DNA cleavage activities ofCo[C₂₅H₁₃N₃O₆H₂O],Ni[C₂₅H₁₃N₃O₆H₂O]and Cu[C₂₅H₁₃N₃O₆H₂O]complexesareanalyzedutilizinga garose gel electrophoresis techniquecontrary to DNA of *E.Coli*. DNA-binding research places a strong emphasis on the rational design and development of innovative, more effective drugs that target DNA [53].

		
Marker:Standard Molecular weight Marker; Control- DNA of <i>E. Coli</i> ; Lane D1: <i>E.coli</i> DNA treated with Schiff base I Lane D2: <i>E.Coli</i> DNA treated with Co[C ₂₅ H ₁₃ N ₃ O ₆ H ₂ O] Lane D3: <i>E.Coli</i> DNA treated with Ni[C ₂₅ H ₁₃ N ₃ O ₆ H ₂ O] Lane D4: <i>E.coli</i> DNA treated with Cu[C ₂₅ H ₁₃ N ₃ O ₆ H ₂ O]	M: Standard Molecular weight Marker; C- Control DNA; <i>P. aeruginosa</i> Lane 1: <i>P. aeruginosa</i> Schiff base I Lane 2: <i>P. aeruginosa</i> DNA treated with Co[C ₂₅ H ₁₃ N ₃ O ₆ H ₂ O] Lane 3: <i>P. aeruginosa</i> DNA treated with Ni[C ₂₅ H ₁₃ N ₃ O ₆ H ₂ O] Lane 4: <i>P. aeruginosa</i> DNA treated with Cu[C ₂₅ H ₁₃ N ₃ O ₆ H ₂ O]	Marker: Standard Molecular weight Marker; Control- DNA of <i>A. niger</i> ; Lane D1: <i>A. niger</i> DNA treated with Schiff base I; Lane D2: <i>A. niger</i> DNA treated with Co[C ₂₅ H ₁₃ N ₃ O ₆ H ₂ O] Lane D3: <i>A. niger</i> DNA treated with Ni[C ₂₅ H ₁₃ N ₃ O ₆ H ₂ O] Lane D4: <i>A. niger</i> DNA treated with Cu[C ₂₅ H ₁₃ N ₃ O ₆ H ₂ O]
Figure 5A: DNA Cleavage studies of <i>E. Coli</i>	Figure 5B: DNA Cleavage studies of <i>P. aeruginosa</i>	Figure 5C: DNA Cleavage studies of <i>A. niger</i> .

The electrophoresis exposed the reaction of metal complexes on DNA takes place when there exists the molecular weight variation. Among the control and treated DNA sample, the variation was found in the bands of Lane 1-3, in contrast to the control DNA of *E. coli* (Fig. 5A), *P. aeruginosa* (Fig. 5B) and *A. niger* (Fig. 5C). Thus, observation suggests that control DNA by itself fails to demonstrate any fragmentation in comparison with complexes. Nevertheless, the actions of chemical intercede implicated in the complex DNA fragmentation has not been analyzed. The DNA cleavage compounds in the development of pathogenic organisms by hewing the genome. The distinct binding affinity with DNA enhances the DNA cleavage efficiency. We conclude that the complexes $\text{Co}[\text{C}_{25}\text{H}_{13}\text{N}_3\text{O}_6\text{H}_2\text{O}]$, $\text{Ni}[\text{C}_{25}\text{H}_{13}\text{N}_3\text{O}_6\text{H}_2\text{O}]$ and $\text{Co}[\text{C}_{25}\text{H}_{13}\text{N}_3\text{O}_6\text{H}_2\text{O}]$ (Fig. 5A: lane 1, 2 and 3 respectively) cleave DNA in contrast to control DNA. Figure 5A shows the differences in the Lane 1-3 bands compared to the *E. coli* control DNA. Conelly J. C. and associates investigated DNA breakage and degradation by the SbcCD protein complex from *E. coli* [54]. Fig. 5B exposes the bands of Lane 1-3 in contrast to the control DNA of *P. aeruginosa*. Hence, the control DNA alone fails to exhibit apparent cleavage and is achieved by the Schiff base and its complexes. Teesta Jain and coworkers investigated how PAT relaxes positively and negatively supercoiled DNA [55]. N. Raman et al. investigated the DNA cleavage and antibacterial and antifungal properties of transition metal complexes containing 4-Aminoantipyrine byproducts of N_2O_2 type structures with *P. aeruginosa* [56]. Nada Kraevac and colleagues investigated DNA cleavage with the Glucoamylase-TNF Fusion Protein Secreted from *Aspergillus niger* [57]. As a result, research revealed that the control DNA alone does not display apparent cleavage, which is accomplished by the Schiff base and its complexes.

3.9 Antioxidant studies

The radical quenching capacity of the compounds and positive standards (BHA and ascorbic acid) were evaluated spectrophotometrically in the DPPH test. In broad sense, the complex reduces the stable radical DPPH to the yellow-colored DPPH-H with IC_{50} values varying from $139 \pm 1.71 \mu\text{g/ml}$ to $276 \pm 3.01 \mu\text{g/ml}$ (Figure 6).

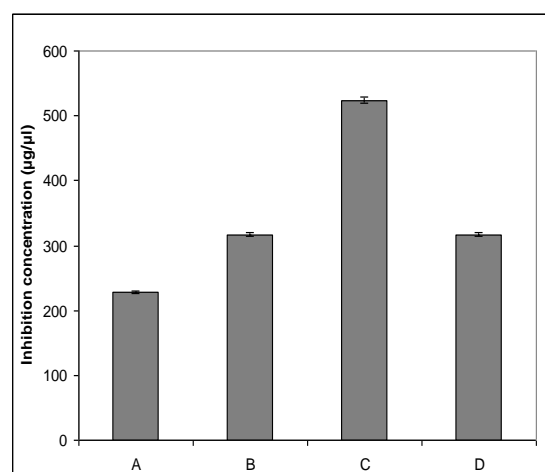


Fig.6:Antioxidant studies; Inhibition of DPPH. Schiff base(A), Co (II) (B), Ni (II)(C) and Cu (II) (D) complexes.

As positive standards, BHA and ascorbic acid demonstrated strong antioxidant activity, with corresponding IC_{50} values of 4.25 and 5.66 $\mu\text{g/ml}$. The substrate $\text{C}_{27}\text{H}_{19}\text{N}_3\text{O}_6$ had the lowest IC_{50} activity of 229 ± 1.91 , whereas the compounds of the same molecule $\text{Co}[\text{C}_{25}\text{H}_{13}\text{N}_3\text{O}_6\text{H}_2\text{O}]$, $\text{Ni}[\text{C}_{25}\text{H}_{13}\text{N}_3\text{O}_6\text{H}_2\text{O}]$, and $\text{Cu}[\text{C}_{25}\text{H}_{13}\text{N}_3\text{O}_6\text{H}_2\text{O}]$ had greater activity of 317 ± 2.17 , 524 ± 4.21 and $317 \pm 2.31 \mu\text{g/ml}$, accordingly. Figure 8 signposts the nearly identical replications of radical scavenging activity with mean \pm standard error. Muzaffer Alkan and his contemporaries investigated the antioxidant activity of triazole compounds [58]. The recent investigation shows that the class of polyphenolic substances such as flavonoids also forms the metal clusters. Furthermore, studies also signify that when flavonoids are linked with transition metal ions, their antioxidant action increases [59].

3.10 Molecular Docking

Docking studies were conducted on a series of coumarin analogues synthesized against the VEGFR2 enzyme in order to better understand the hydrophobic, hydrogen bonding, and electrostatic interactions between ligands and amino acid residues found in the active pocket of VEGFR2. To analyse ligand binding orientations, we used molecular docking tools such as PyMol (TM) 2.3.4, Biovia-Discovery Studios 2021 Client, PyRx, and USCF Chimaera 1.14. PDB ID 3EWH refers to the X-ray structure of the VEGFR2 protein, which was obtained along with a co-crystallized pyridyl-pyrimidine benzimidazole analogue.

The docked ligands demonstrated strong binding affinities with a protein, with binding unconstrained energies ranging from -9.7 to -11.6 kcal/mol. The binding energy value represents the degree to which a ligand and receptor interact. The **Co** metal complex of coumarin analogue interacted with the amino acids of ARG1051, ASP1056, and LEU889 *via* electrostatic interactions with a π -cation, π -anion unfavorable positive-positive, unfavourable interactions between donors and π -sigma. The **Co** metal complex of coumarin is also exhibited a hydrophobic interaction with the amino acids ALA881, and ILE888 *via* π -alkyl bond interactions.

The **Cu** metal complex interacted with the ARG1051, ASP1056, and LEU889 amino acid

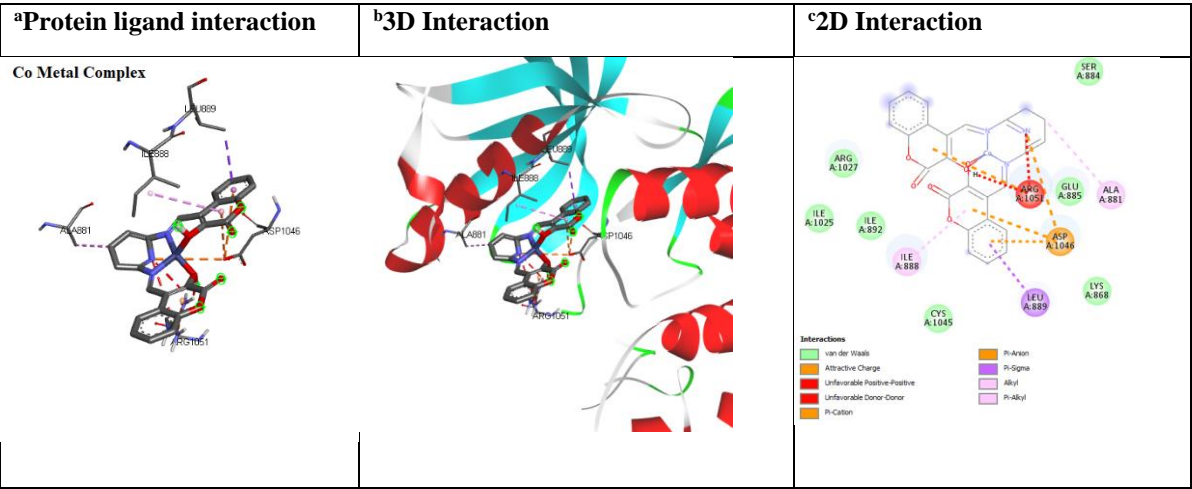
residues *via* π -cation, π -anion unfavorable positive-positive, unfavourable interactions between donors and π -sigma(electrostatic interactions) and with the amino acids ALA881, and ILE888 *via* π -alkyl bond interactions (hydrophobic interactions). The **Ni** metal complex of coumarin exhibited a hydrogen bond contact through conventional and carbon-hydrogen bond interactions with the amino acid residues ARG1051 and GLU885.

The amino acids ASP1046, and CYS1024 involved in the electrostatic bond interactions with the **Ni** metal complex of coumarin *via* π -cation, π -anion, and π -sulphurinteractionsand with the amino acids ALA881, and ILE888 *via* π -alkyl bond interactions (hydrophobic interactions) (Table 01 & Fig 01).

Table 01: Molecular docking result of compounds 9(a-e) with VEGFR2 (PDB ID: 3EWH)

Entry	^a BA (Kcal/mol)	Interacting residues				
		^c HB	^d HB length Å°	^e EI	^f Hydrophobic and other interaction	
Co	-11.6	-	-	ARG1051, ASP1046 LEU886	ALA881, ILE888	
Cu	-11.2	-	-	ARG1051, ASP1046 LEU886	ALA881, ILE888	
Ni	-9.7	ARG1051 GLU885	2.32, 6.08 3.24	CYS1024, ARG1051	ALA881, ILE888	

^aBA: Binding affinity., ^cHB: Hydrogen bonds., ^dHydrogen bond length in Å°, ^eElectrostatic interactions., ^fOther hydrophobic interactions between **9a-e** and protein.



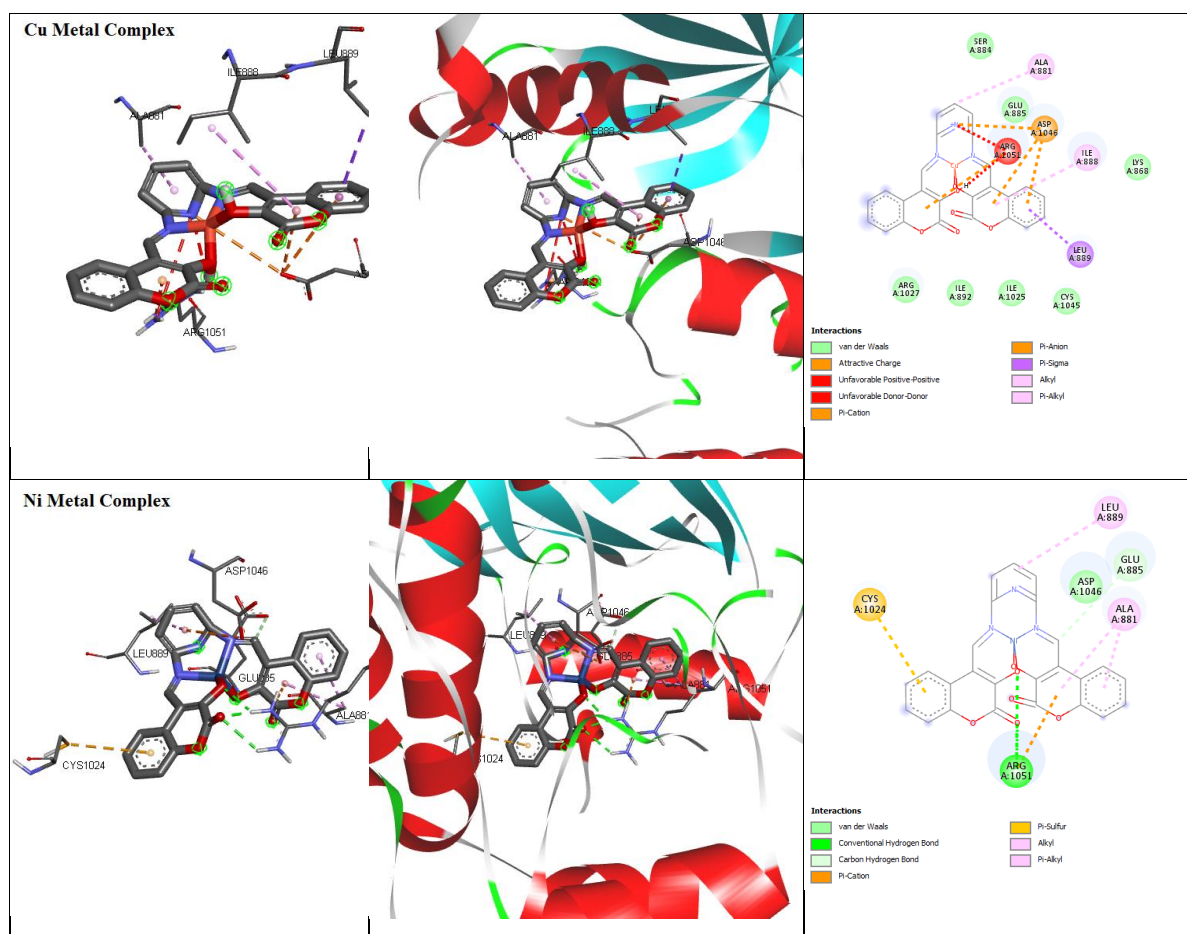


Fig 01: ^aMetalcomplexs interacted with amino acid residues showing hydrogen bond, electrostatic and hydrophobic interactions, ^b3-Dimensional/^c2—Dimensional visuals interaction of ligands with VEGFR2 (PDB ID: 3EWH).

When the AMBER force field is used in combination with the UCSF-Chimera 1.14 software, the quantities of the protein and ligand may be greatly decreased. VEGFR2 complexing with pyridyl-pyrimidine benzimidazole analog's protein structure may be found in the Protein Data Bank (PDB ID: 3EWH). The protein's odd residues were removed, and the AMBER force field significantly reduced them. After adjusting the PyRX workstation's grid box dimensions to x: 24.77, y: 23.24, and z: 24.00, the ligands were precisely docked at the binding site. The docked findings were assessed using the PyRx simulated screening program, and the results were displayed by the matching binding affinity values. The PDB data for the ligand and protein were combined using PyMol. The program Biovia Discovery Studios enables the viewing of generated figures in three dimensions.

Conclusion

The freshly synthetic Schiff bases function as polydentate ligands, interacting with metal ions by means of deprotonation of the azomethine nitrogen and phenolic oxygen atoms. Some antimicrobial and antifungal species were reported to be extremely potent against Schiff bases and its metal compounds. The substantial raise in activity found due to co-ordination. The DNA cleavage experiments indicated the compounds exhibited non-specific DNA cleavage activity. All compounds and combinations are investigated by determining its antioxidant properties. These results urge us to suggest the structure layout depicted in **Fig.7**.

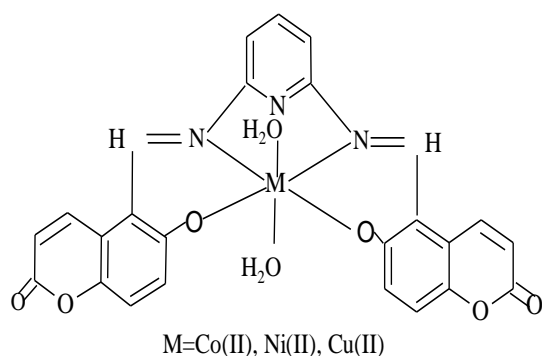


Fig.7:Structure of metal complex.

Acknowledgment

The authors are thankful to BIET, Davanagere

Conflict of Interest

The authors do not have any conflict of interest

Data Availability Statement

All data set used in this research work is available based on request.

References

1. R.D. Murray and J. Mendez, Brown SA, The Natural Coumarins: Occurrence, Chemistry and Biochemistry, Wiley-Interscience, New York. 1982. 1-12.
2. D.Egan, R.O'Kennedy, E.Moran, D.Cox, R.D.Thornes, The pharmacology, metabolism, analysis, and applications of Coumarin coumarin-related compounds, Drug Metab Rev. 22 503 (1990).
3. T. Mihaylov, N. Trendafilova, I. Kostava, I. Georgieva and G. Bauer. DFT modelling and spectroscopic study of metal-ligand bonding in La (III) complex of coumarin-3-carboxylic acid, Chemical Physics. 327, 209 (2006)
4. IP Kostova, I. Manolov, I. Nicolova and N. Danchev, New metal complexes of 4-methyl-7-hydroxycoumarin sodium salt and their pharmacological activity, Farmaco. 56, 707 (2001).
5. F.A. Jimenez-Orozco, J.A. Molina-Guarneros, N. Mendoza-Patino, F. Leon-Cedeno, B. Flores-Perez, E. Santos-Santos and J.J. Mandoki. The cytostatic activity of coumarin metabolites and derivatives in the B16-F10 murine melanoma cell line Melanoma, Res. 9, 243 (1999).
6. G.J. Finn, B.S. Creaven, and D.A. Egan. Study the in vitro cytotoxic potential of natural and synthetic coumarin derivatives using human normal and neoplastic skin cell lines Melanoma, Res. 11, 461 (2001).
7. P. Laurin, M. Klich, C. Dupis-Hamelin, P. Mauvais, P. Lassaigne, A. Bonnefoy and B. Musicki. Synthesis and in vitro evaluation of novel Highly potent coumarin inhibitors of gyrase B, Bioorg. Med. Chem. Lett. 9, 2079 (1999).
8. R.J.S. Hoult and M. Paya. Pharmacological and biochemical actions of Simple coumarins: Natural products with therapeutic potential, Gen. Pharmacol. 27, 713 (1996).
9. S.P. Pillai, S.R. Menon, L.A. Mitscher, C.A. Pillai, and D.A. Shankel. Umbelliferone Analogues and Their Potential to Inhibit Benzo(a)pyrene- and Hydrogen Peroxide-Induced Mutations, J. Nat. Prod. 62, 1358, (1999).
10. Y. Kimura, H. Okuda, S. Arichi, K. Baba, and M. Kozawa, Inhibition of the formation of 5-hydroxy-6,8,11,14-eicosatetraenoic acid from arachidonic acid in polymorphonuclear leukocytes by various coumarins, Biochim. Biophys. Acta. 834, 224 (1985).
11. G.J. Finn, B.S. Creaven, D.A. Egan and S.C. Bernadette, In vitro Cytotoxic potential and mechanism of action of selected coumarins, using human renal cell lines. 61, 183 (2002).
12. G.J. Finn, B.S. Creaven and D.A. Egan, A study of the role of cell cycle events mediating the action of coumarin derivatives in human malignant melanoma cells, Cancer Lett. 43, 214 (2004).
13. G.J. Finn, B.S. Creaven and D.A. Egan, Activation of mitogen-activated protein kinase pathways and melanogenesis by novel nitro-derivatives of 7-hydroxy coumarin in human malignant melanoma cells Eur. J. Pharm. Sci. 16, 26 (2005).

14. R. Kennedy, R.D. Thornes, Coumarins: Biology, Applications and Mode of Action, John Wiley & Sons, Chichester, 1997.
15. M. Zabradnik, The Production and Application of Fluorescent Brightening Agents, John Wiley & Sons, New York, 1992.
16. R.D.H. Murray, J. Mendez and S.A. Brown, The Natural Coumarins: Occurrence, Chemistry and Biochemistry, John Wiley & Sons, New York, 1982.
17. H. von Pechmann and C. Duisberg. Chem. Ber. 17, 929 (1884).
18. J.R. Johnson, Org. React. 1, 210 (1942).
19. G. Jones, Org. React. 15 204 (1967).
20. G. Brufola, F. Fringuelli, O. Piermatti and F. Pizzo, Heterocycles. 43, 1257 (1996).
21. R.L. Shriner, Org. React. 1, 1 (1942).
22. I. Yavari, R. Hekmat-Shoari and A. Zonouzi, A New and Efficient Route 4-Carboxymethylcoumarins Mediated by Vinyltriphenyl phosphonium Salt, Tetrahedron Lett. 39, 2391 (1998).
23. J. Liu, T. Zhang, T. Lu, L. Qu, Zhou, Q. Zhang and L. Ji. DNA-binding and cleavage studies of macrocyclic copper (II) complexes. Inorg. Biochem. 91, 269 (2002).
24. P. Marguerite, J.C. Burrows and B. Meunier. Mechanisms of DNA Cleavage by copper complexes of 3-Clip-Phen and its conjugate with a distamycin analogue 28, 4856 (2000).
25. P.R. Reddy, K.S. Rao and Satyanarayana B. Synthesis and DNA Cleavage properties of ternary Cu (II) complexes containing histamine and amino acids Tetrahedron Lett. 47, 7311 (2006).
26. J. Baumann, G. Wurn, V. Bruchlaussen and N.S. Prostaglandin Synthetase inhibiting O₂-radical scavenging properties of some flavonoids and related phenolic compounds. Arch. Pharmacol. 27, 308 (1979).
27. G.B. Bagihalli, P.G. Avaji, S.A. Patil and Badami P.S. Synthesis, spectral characterization, in vitro antibacterial, antifungal and cytotoxic activities of Co (II), Ni (II) and Cu (II) complexes with 1,2,4-triazole Schiff bases, Eur. J. Med. Chem, 43, 2639 (2008).
28. Bhushan S. Sail, Vinod H. Naik, B.M. Prasanna, Naushad Ahmad, Mohammad Rizwan Khan, M.R. Jagadeesh, Ravikumar Cheedarala. Synthesis, characterization and pharmacological studies of cobalt (II), nickel (II) and copper (II) complexes of thiazole schiff bases J. Mol. Struct. 1288 (2023) 135748.
29. A.D. Kulkarni, S.A. Patil, P.S. Badami, SNO donor Schiff bases and their Co (II), Ni (II) and Cu (II) complexes: synthesis, characterization, electrochemical and antimicrobial studies J. Sulfur Chem. 2009; 30: 145.
30. V.K. Ahluwalia, P. Bhagat, R. Aggarwal, R. Chandra, Intermediates for organic synthesis IK International Pvt. Ltd. Delhi. 2005.
31. E. Spath, M. Pailer, Chem. Ber. 1935; 68: 940.
32. A.D. Kulkarni, G.B. Bagihalli, S.A. Patil, P.S. Badami, Synthesis, characterization, electrochemical and in-vitro antimicrobial studies of Co (II), Ni (II), and Cu (II) complexes with Schiff base of formylcoumarin derivatives J. Coord. Chem. 2009; 62: 3060.
33. Bhushan S. Sail, Vinod H. Naik, Majid Rasool Kamli, B. M. Prasanna, Synthesis, spectral, in vitro microbial and DNA cleavage studies of isatin bis hydrozone metal complexes J. Mol. Struct. 1277 (2023) 134837.
34. Naik RM, Thakor VM, Formylation of Benzopyrones. I. Formylation of Hydroxycoumarins with Hexamethylenetetramine Current Sci. 1957; 22: 1626.
35. K. S. Manjunatha, N. D. Satyanarayan, S. Harishkumar. Antimicrobial and *in silico* ADMET screening of Novel (E)-N-(2-(1H-indol-3-yl-amino) vinyl)-3-(1-methyl-1H-indol-3-yl)-3

- Phenylpropanamidederivatives *Int. J. Pharm. Sci.* 8(10):251-256.
36. Blois MS, Antioxidant Determinations by Using a Stable Free Radical Nature. 1958; 26: 1199.
 37. İlhan S, Temel H, Yılmaz I, Sekerci M, Synthesis, structural characterization and electrochemical studies of new macrocyclic Schiff base containing pyridine head and its metal complexes. *Journal of Organometallic Chem.* 2007; 692: 3855.
 38. Shyamala BS, Ananthalakshmi PV, Raju VJT, Rao PN, Reddy PUM. Antifeeding and insect-growth-regulating activity of certain metal complexes towards *Spodoptera litura* *Biomaterials*. 1992; 5: 23.
 39. Aazam ES, E Husseiny AF, Hitchcock P.B. Alshehri J.M. A dimeric copper coumarin complex synthesis and crystal structure of $[Cu(4\text{-methyl-7-(salicylideneamino)coumarin})_2]_2$ *Cent. Eur. J. Chem.* 2008; 6: 319–323.
 40. Refat MS, El-Deen IM, Anwer ZM, El-Ghol S.. Bivalent transition metal complexes of coumarin-3-yl thiosemicarbazone derivatives: Spectroscopic, antibacterial activity and thermogravimetric studies *Journal of Molecular Structure* 2009; 920: 149.
 41. Nabil Youssef S, El-Zahany E, Ahmed El-Seidya MA, Caselli A, Cenini S. *Journal of Molecular Catalysis A Chemical*. 2009; 34: 905.
 42. Singh K, Barwa MS, Tyagi P. Synthesis, characterization and biological studies of Co(II), Ni(II), Cu(II) and Zn(II) complexes with bidentate Schiff bases derived by heterocyclic ketone *Eur. J. Med. Chem.* 2006; 41: 14.
 43. Rama Krishna Reddy K, Mahendra KN. Synthesis, Characterization, and the Antimicrobial and Anthelmintic Activities of some Metal Complexes with a New Schiff base 3-[(Z)-5-Amino-1,3,3-Trimethyl Cyclohexylmethylimino]-1,3-Dihydroindol-2-One *Russian Journal of Inorganic Chemistry*, 2008; 53: 906–912.
 44. Patil S.A, Naik, V.H. A.D. Kulkarni, P.S. Badami, DNA cleavage, antimicrobial, spectroscopic and fluorescence studies of Co(II), Ni(II) and Cu(II) complexes with SNO donor coumarin Schiff bases, *Spectrochimica Acta Part A: Molecular and Biomolecular Spectroscopy*. 2010; 76.
 45. El-Sawaf AK, West DX, El-Saied FA, RM El-Bahnasawy, Synthesis, magnetic and spectral studies of iron (III), cobalt (II, III), nickel (II), copper (II) and zinc (II) complexes of 4-formylantipyrine N (4)-antipyrinylthiosemicarbazone. *Trans. Met. Chem.* 1998; 649: 23.
 46. Saha N, Mukherjee N. *Polyhedron* 1984; 3: 1135.
 47. Gupta LK, Chandra S. Spectroscopic characterization and EPR spectral studies on transition metal complexes with a novel tetradentate, 12-membered macrocyclic ligand. *Spectrochim. Acta Part A*. 2006; 65: 792.
 48. Angelusiu MV, Barbuceanu SF, Draghiciand C, Almajan GL. New Cu (II), Co (II), Ni (II) complexes with aroyl-hydrazone based ligand. Synthesis, spectroscopic characterization and in vitro antibacterial evaluation. *European Journal of Medicinal Chemistry*. 2010; 45: 2055.
 49. Singh DP, Kumar R, Malik V, Tyagi P. Synthesis, spectral, and antibacterial studies of 16-membered tetraazamacrocyclic complexes, *Trans. Met. Chem.* 2007; 32: 1051.
 50. Chandra S, Verma S. synthesis, spectral, and antifungal studies of transition metal complexes with sixteen-membered hexadentate macrocyclic ligand *Russian J. Coord. Chem* 2008; 34: 499.
 51. Neelakantana MA, Rusalraj F, Dharmaraja J, Johnsonraja S, Jeyakumarb T, Sankaranarayana Pillai M. *Spectrochimica Acta Part A*. 2008; 71: 1599.
 52. Chohan ZH, Scozzafava A, Supuran CT. Metal binding and antibacterial activity of

- ciprofloxacin complexes, J EnzInhib Med Chem2005; 18: 303.
53. Waring, M.J. Drug Action at the Molecular Level, G.C.K. Roberts Ed. Maemillar London (1977) 167.
54. Conelly JC, de Leau ES, Leach DR. DNA cleavage and degradation by the SbcCD protein complex from *Escherichia coli*, Nucleic acids Res. 1999; 27: 1039.
55. Jain T, Roper BJ, Anne G. A functional type I topoisomerase from *Pseudomonas aeruginosa* BMC Molecular Biology. 2009; 10: 23.
56. Ramana N, Mitub L, Sakthivela A, Pandia MSS. Studies on DNA cleavage and Antimicrobial Screening of Transition Metal Complexes of 4-Aminoantipyrine Derivatives of N₂O₂ Type J. Iran. Chem. Soc. 2009; 6: 738., 1 (2009), 1